TECHNICAL STUDY · ANALOG PLAYBACK

# Mechanical, geometric and electrical interfacing of tonearm and cartridge

Dynamics of the playback system, alignment geometries, fine adjustments and electrical interfacing with the phono stage

## Introduction

Playing a phonograph record is a multistage transduction process in which each element of the chain imposes boundary conditions on the one that follows. The information is cut as a geometric modulation of the groove: the stylus converts it into mechanical motion, the cartridge generator into an electrical voltage, and the input circuit of the phono stage, together with the wiring, determines the final response. Cartridge, tonearm, cable and preamplifier must therefore be evaluated as a single system, because their characteristic quantities (mass, compliance, geometry, inductance, capacitance, load resistance) interact with one another.

The first domain is mechanical. The tonearm-cartridge assembly behaves as a second-order damped oscillator, in which the effective mass of the tonearm, referred to the stylus tip, and the viscoelastic compliance of the suspension set a fundamental resonance frequency. The position of this resonance relative to the record warps and to the lower end of the audio band, together with the degree of damping, determines tracking stability before the characteristics of the transducer even come into play.

The second domain is kinematic. The cutting lathe's stylus cuts the groove while moving along a radius, whereas a pivoted tonearm describes a circular arc: the result is an angular tracking error that can only be distributed across the side of the record. The classical alignment geometries (Loefgren A/Baerwald, Loefgren B, Stevenson) are solutions of the same optimization problem and differ in the criterion by which they weight the residual error. To these are added the fine adjustments (tracking force, anti-skating compensation, vertical tracking angle and azimuth), which govern the contact between the diamond and the groove walls.

The third domain is electromagnetic. The cartridge generator, which is velocity-sensitive, presents an internal impedance that forms a second-order network with the wiring capacitance and with the input impedance of the phono stage. In moving-magnet and moving-iron cartridges, which have high inductance, this network resonates in the upper part of the audio band and must be dimensioned together with the mechanical response of the stylus. In low-impedance moving-coil cartridges the resonance shifts into the radio-frequency range, and the resistive load, applied directly or reflected by a step-up transformer, acts mainly on damping and on the signal-to-noise ratio.

The study addresses the three domains in this order, with an intermediate chapter on the structural resonances of the armtube and headshell. The executive summary that follows condenses the results; the subsequent chapters develop the physical models and equations, while the two appendices collect the analytical derivations of the alignment geometries and the numerical application to real combinations of tonearms and cartridges.

## Executive Summary (TL;DR)

- **Mechanical Modeling:** The cartridge-tonearm system is a second-order damped harmonic oscillator (mass-spring-damper). The total effective mass interacts with the dynamic compliance of the elastomer to produce a fundamental resonance that must be confined between 8 Hz and 12 Hz (ideal target: 9–11 Hz).
- **Moment of Inertia:** The effective mass of the tonearm does not coincide with its static mass but depends on the radial distribution of the masses relative to the pivot ($I = \Sigma\, m_i \cdot r_i^2$).

- **Kinematics and Alignment:** Pivoted tonearms introduce an angular tracking error that generates second-harmonic distortion inversely proportional to the groove radius. The Loefgren A (Baerwald), Loefgren B and Stevenson geometries optimize the distribution of the weighted error by means of two zero-error points (null points).
- **Tribology and Vector Forces:** Tracking is governed by the vertical preload (VTF), by the inward skating force related to dynamic friction and to the offset angle, by the vertical tracking angle (VTA/SRA), and by the axial symmetry in the groove (azimuth).
- **Electrical Interfacing:** MM/MI cartridges (high inductance) form a second-order LC resonant circuit with the cable and preamplifier capacitance in the upper audio band (10–20 kHz). Low-output MC cartridges (low inductance and very low internal impedance) show ultrasonic electrical resonances (MHz) and operate in a resistive regime (voltage coupling, Lenz electrodynamic damping, or current coupling with transimpedance amplifiers or step-up transformers).

## 1. Physical Modeling and Mechanical Dynamics

### 1.1 The Second-Order System (Mass-Spring-Damper)

From the standpoint of rational mechanics, the assembly formed by the tonearm, the cartridge body and the moving system (cantilever + elastomer suspension) behaves as a vibrating system with one degree of freedom in each of the two orthogonal planes (horizontal/lateral and vertical).

- **Below the resonance frequency ($f < f_0$):** The suspension behaves as a rigid connection. The tonearm follows the groove profile (record undulations or warp) entirely, with no relative deflection between cantilever and cartridge body; the electrical output tends to zero (mechanical high-pass filter at 12 dB/octave).
- **At the resonance frequency ($f = f_0$):** The mechanical energy transferred to the system undergoes an amplification that depends on the quality factor Q. If poorly damped, the cantilever excursion reaches the elastic limit, modulating the instantaneous tracking force until contact is lost (mistracking).
- **Above the resonance frequency ($f > f_0$):** The inertia of the total mass keeps the tonearm and cartridge body stationary with respect to the high-frequency modulations. The stylus follows the groove undulations and transmits the relative motion in full to the magnetic generator.

### 1.2 Differential Equation of Motion and Fundamental Frequency ($f_0$)

The differential equation governing the relative motion z(t) between the stylus (excited by the groove x(t)) and the total effective mass $M_{tot}$ is:

$$M_{tot} \cdot (d^2z / dt^2) + R_m \cdot (dz / dt) + (1 / C_{dyn}) \cdot z = -M_{tot} \cdot (d^2x / dt^2)$$

Where:

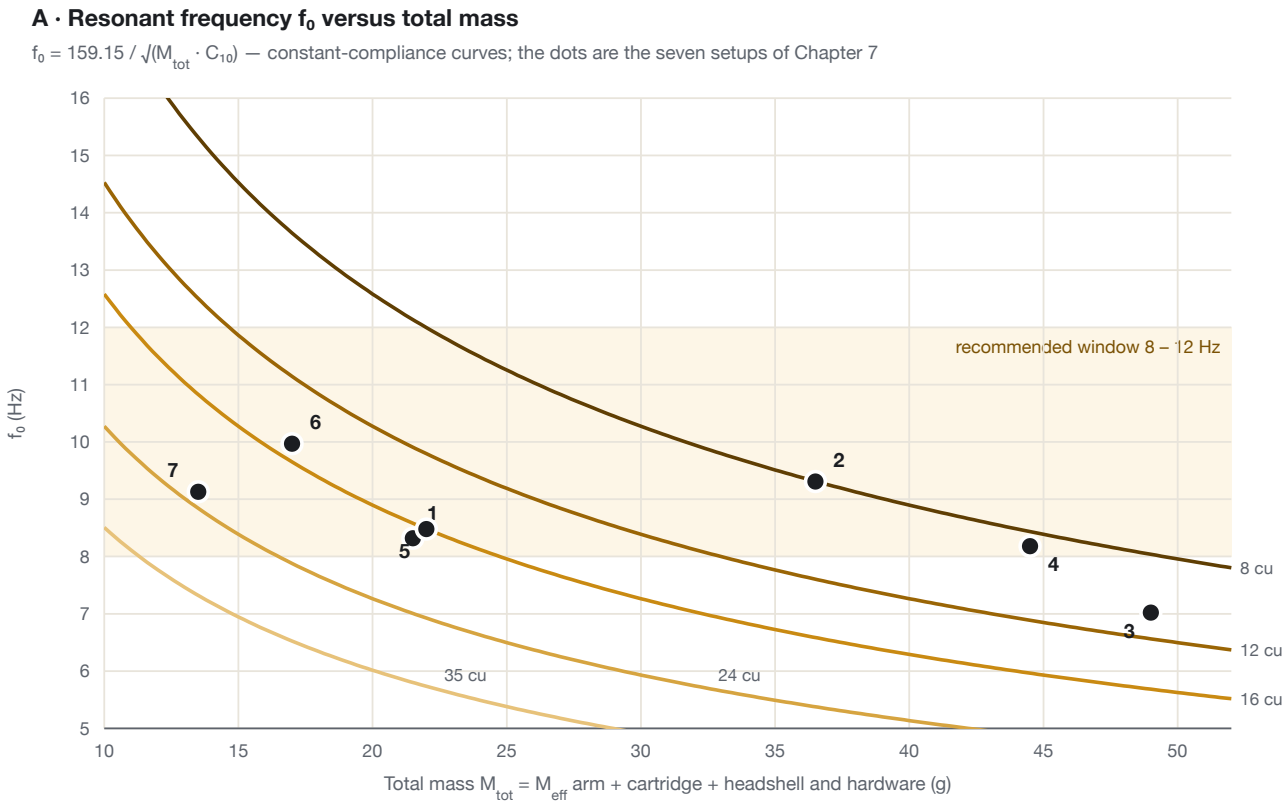
- **$M_{tot}$:** Total effective mass referred to the stylus tip, expressed in grams (g) or kilograms (kg). It is given by the sum: $M_{tot} = M_{eff}$ (effective mass of the tonearm) + $M_c$ (mass of the cartridge) + $M_h$ (mass of screws, nuts, washers and spacers).
- **$R_m$:** Viscous mechanical resistance of the suspension elastomer (N·s/m).
- **$C_{dyn}$:** Dynamic compliance (the inverse of the spring constant k, $C_{dyn} = 1/k$), expressed in μm/mN (equivalent to $10^{-6}$ cm/dyne or "cu" - compliance units).

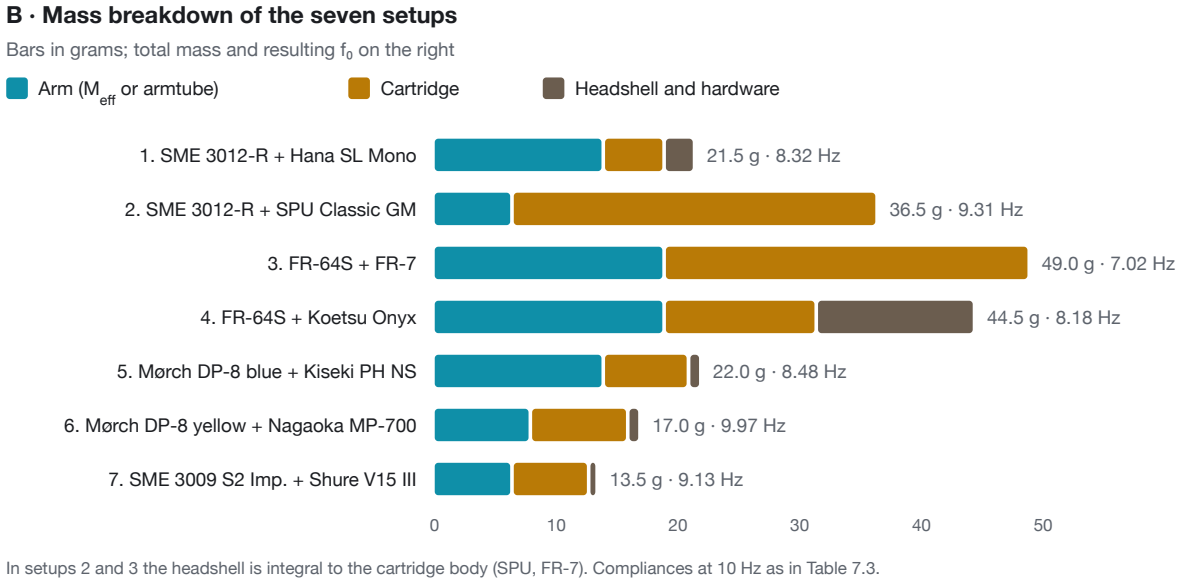
From the natural angular frequency $\omega_0 = 1 / \sqrt{(M_{tot} \cdot C_{dyn})}$, the standard engineering formula follows:

$$f_0 = 1 / (2\pi \cdot \sqrt{(M_{tot} \cdot C_{dyn})}) \approx 159.155 / \sqrt{(M_{tot} \cdot C_{dyn})} \text{ [Hz]}$$

The optimal operating window lies between 8 Hz and 12 Hz (nominal target: 9–11 Hz):

- **Lower limit (< 8 Hz):** Overlap with the energy spectrum of the physical undulations of the vinyl (warp spectrum, concentrated between 0.55 Hz and 5 Hz), with turntable bearing rumble and with the resonances of the suspended chassis.
- **Upper limit (> 12 Hz):** Excessive proximity to the lower end of the recorded audio band (20 Hz), with consequent alteration of the phase and amplitude response at low frequencies and mechanical intermodulation.




In setups 2 and 3 the headshell is integral to the cartridge body (SPU, FR-7). Compliances at 10 Hz as in Table 7.3.

***Figure 1*** *— Resonance frequency $f_0$ as a function of total mass, for compliances from 8 to 35 cu (A), and distribution of the mass among tonearm, cartridge and headshell in the seven setups of Table 7.3 (B). The highlighted band is the recommended window of 8–12 Hz.*

### 1.3 Moment of Inertia and Effective Mass of the Tonearm ($M_{eff}$)

The effective mass of a tonearm is not a quantity that can be measured with a static balance (which measures the weight force once the counterweight is unbalanced); it is an inertial quantity derived from the second law of rotational dynamics.
For a tonearm of effective length $L_{eff}$ (the distance between the pivot and the stylus tip), the total moment of inertia about the axis of rotation is:

$$I = \int r^2 \, dm \approx \Sigma \, (m_i \cdot r_i^2)$$

The equivalent effective mass concentrated at the stylus is defined as:

$$M_{eff} = I / (L_{eff})^2 = [\, I_{armtube} + M_{headshell} \cdot L_{eff}^2 + M_{cw} \cdot R_{cw}^2 \,] / L_{eff}^2$$

Design and operating consequences:

- **Position and mass of the counterweight ($M_{cw}$):** To balance the tonearm statically, the front and rear torques must be equal ($M_{front} \cdot L_{eff} = M_{cw} \cdot R_{cw}$). However, since the moment of inertia depends on the square of the distance ($R_{cw}^2$), a heavier counterweight placed very close to the pivot sharply reduces $R_{cw}^2$, lowering the overall effective mass of the system compared with a lighter counterweight placed far from the pivot.
- **Changing armtube or headshell:** Mass added at the headshell ($r \approx L_{eff}$) contributes to the total effective mass in a 1:1 ratio, whereas mass distributed along the armtube contributes about 1/3 of its static mass (for a uniform cylinder pivoted at one end, $I = 1/3 \cdot m \cdot L^2$).
- **Horizontal-Vertical Asymmetry:** In short-carriage tangential tonearms, or in pivoted tonearms with eccentric masses or asymmetric joints (e.g. vertical-only knife-edge bearings and an offset horizontal pivot), the horizontal effective mass $M_{eff,H}$ differs from the vertical one $M_{eff,V}$, giving rise to two distinct resonance frequencies $f_0$,H and $f_0$,V.

### 1.4 Viscoelastic Behavior of the Elastomer and 100 Hz → 10 Hz Conversion

The suspension rubber (damper made of butyl or synthetic elastomers) is not an ideal spring but a nonlinear viscoelastic element whose complex shear modulus $G^*(\omega) = G'(\omega) + jG''(\omega)$ increases with frequency.

- **European/US Standard (10 Hz):** The dynamic compliance is measured directly at 10 Hz, making the figure immediately usable in the $f_0$ formula.
- **Japanese JIS Standard (100 Hz):** Manufacturers such as Denon, Audio-Technica, Nagaoka and Fidelity Research specify the dynamic compliance measured at 100 Hz ($C_{100}$). At 100 Hz the elastomer shows a markedly higher dynamic stiffness than at 10 Hz.
- **Empirical conversion relation:**

$$C_{10} \approx k_{conv} \cdot C_{100}$$ *(with $k_{conv}$ between 1.5 and 2.0, typical mean value = 1.75)*

*Note on methodological rigor:* The factor $k_{conv}$ is not a universal physical constant, since it depends on the chemical formulation of the elastomer, the age of the suspension and the operating temperature (variations of ±5 °C from the standard 20 °C shift the compliance significantly). Instrumental verification with a test record remains the only exact method.

### 1.5 Quality Factor (Q) and Fluid Damping

The mechanical quality factor at resonance is defined as:

$$Q_m = [\, \sqrt{(M_{tot} / C_{dyn})} \,] / R_m$$

- A high value of $Q_m$ (> 3, corresponding to a peak > +9.5 dB at $f_0$) results in prolonged oscillation of the tonearm after an impulse or a warp, causing Doppler intermodulation (frequency modulation of the audio signal due to the longitudinal oscillation of the stylus in the groove) and cyclic variations of the VTF.

- **Damping with silicone fluid:** Fitting a trough containing a high-kinematic-viscosity silicone fluid (e.g. dimethylpolysiloxane from 30 000 cSt to 200 000 cSt), in which a paddle attached to the tonearm is immersed, introduces an external viscous resistance $R_{ext}$ proportional to the angular velocity ($F_d = -R_{ext} \cdot dz/dt$). At audio frequencies ($f > 20$ Hz), where the displacement amplitude of the tonearm is infinitesimal, the fluid is transparent; at the frequency $f_0$ (large motion amplitudes), the fluid dissipates thermal energy, suppressing the resonance peak and reducing $Q_m$ toward 0.7–1.0 (critical damping corresponds to $Q_m = 0.5$; $Q_m \approx 0.707$ is the Butterworth alignment, with maximally flat response).

### 1.6 Coupling Table: Tonearm and Cartridge Archetypes

| System Category | Tonearm Effective Mass ($M_{eff}$) | Cartridge Compliance at 10 Hz ($C_{10}$) | Historical and Modern Reference Examples | Typical Total Mass ($M_{tot}$) | Resulting $f_0$ |
|---|---|---|---|---|---|
| **Ultra-Low Mass / High Compliance** | 4 g – 8 g | 20 – 45 µm/mN | Tonearms: SME 3009 S2 Improved (fixed headshell), Mørch DP-8 (green/red armtube), Infinity Black Widow.<br>Cartridges: Shure V15 Type III/IV, Ortofon OM30/40. | 11 g – 15 g | 6.1 – 10.7 Hz (extremes of the range) |
| **Medium Mass / Medium Compliance** | 9 g – 14 g | 14 – 22 µm/mN | Tonearms: Rega RB300/RB3000, SME Series V, SME 3012-R, Technics EPA-100, Mørch (yellow/blue armtube).<br>Cartridges: Nagaoka MP-500/700, Hana SL, Lyra Delos. | 18 g – 23 g | 7.1 – 10.0 Hz (extremes of the range) |
| **High Mass / Low Compliance** | 18 g – 35 g | 5 – 11 µm/mN | Tonearms: Fidelity Research FR-64S, Ortofon RMA-309.<br>Cartridges: Ortofon SPU, Fidelity Research FR-7, Denon DL-103, Koetsu Onyx. | 32 g – 50 g | 6.8 – 12.6 Hz (extremes of the range) |

## 2. Kinematics and Tracking Geometry (Pivoted Tonearms)

### 2.1 Origin of Tracking Error and Harmonic Distortion

During mastering, the cutting stylus of the lathe (e.g., Neumann VMS-70/80) moves along a perfectly radial linear guide: the longitudinal axis of the stylus is always perpendicular to the disc radius R (tangent to the groove).
A pivoted tonearm, by contrast, rotates about a fixed pivot and describes a circular arc. As a result, the axis of the cartridge generator forms a lateral error angle $\theta_e$ (Tracking Error Angle) with the groove tangent.

According to the classical treatment by Erik Loefgren (1938) [1] and H.G. Baerwald (1941) [2], the second-harmonic distortion (THD) generated by tracking error for a sinusoidal signal recorded with peak velocity $v_0$ is given by:$THD_2$ (%) $\approx [\, v_0 \cdot |\tan(\theta_e)| / (\Omega_{disc} \cdot R)\, ] \cdot 100 \approx (v_0 / \Omega_{disc}) \cdot [\, |\theta_e\ (\text{rad})| / R\, ] \cdot 100$ ($\Omega_{disc}$ = angular velocity of the disc: 3.49 rad/s at 33⅓ rpm; $v_0$ in mm/s, R in mm)

Because at constant angular velocity (33.33 or 45 rpm) the tangential groove velocity decreases linearly with radius R ($v_t = \omega_{disc} \cdot R$), the physical wavelength cut into the vinyl is compressed toward the inner grooves. The quantity to minimize mathematically is therefore not the absolute angular error $\theta_e$ but the **Weighted Tracking Error (WTE)**:

> **$WTE(R) = |\theta_e(R)| / R$ [degrees/mm or rad/m]**

### 2.2 Fundamental Alignment Equations (Overhang, Offset Angle, Null Points)

To keep $\theta_e$ within fractions of a degree for 9", 10" or 12" arms, two geometric modifications are introduced relative to a straight arm ending at the spindle:

1. **Overhang (O):** The effective length of the arm $L_{eff}$ exceeds the distance between pivot and platter spindle $D_{p2s}$ (Pivot-to-Spindle): $O = L_{eff} - D_{p2s}$.
2. **Offset Angle (α):** The cartridge (or the headshell) is rotated inward by an angle α relative to the line joining the pivot to the stylus tip.

Applying the law of cosines to the triangle formed by the spindle, the tonearm pivot and the stylus tip at a generic groove radius R, the angle between the radius R and the tangent to the arm arc leads to the exact equation for the angular error:

$$\theta_e(R) = \arcsin\left[ (R^2 + L_{eff}^2 - D_{p2s}^2) / (2 \cdot R \cdot L_{eff}) \right] - \alpha$$

Substituting $D_{p2s} = L_{eff} - O$ and defining the constant linear quantity $L_0 = (L_{eff}^2 - D_{p2s}^2) / (2 \cdot L_{eff}) = O \cdot [1 - O / (2 \cdot L_{eff})]$, for small angles (first-order approximation $\sin(x) \approx x$) one obtains: $\theta_e(R) \approx (R / (2 \cdot L_{eff})) + (L_0 / R) - \alpha$

Setting $\theta_e(R) = 0$ yields a second-degree algebraic equation in R whose two real roots are the **Zero-Error Radii (Null Points)** $R_1$ (inner) and $R_2$ (outer):

$$R^2 - (2 \cdot L_{eff} \cdot \sin\alpha) \cdot R + (L_{eff}^2 - D_{p2s}^2) = 0$$

(exact relation: it is the condition $\theta_e = 0$ of the equation with the arcsine)

From the relations between coefficients and roots (Viète's formulas) for the exact equations, the constructional parameters of the arm are obtained as a function of the null points $R_1$ and $R_2$ and the effective length $L_{eff}$ alone:

- **Harmonic Mean of the Null Radii:** $R_{hm} = (2 \cdot R_1 \cdot R_2) / (R_1 + R_2)$
- **Arithmetic Mean of the Null Radii:** $R_{am} = (R_1 + R_2) / 2$
- **Pivot-to-Spindle Distance (exact form):** $D_{p2s} = \sqrt{(L_{eff}^2 - R_1 \cdot R_2)}$. From this follow:
  - **Overhang (O):** $O = L_{eff} - \sqrt{(L_{eff}^2 - R_1 \cdot R_2)} \approx (R_1 \cdot R_2) / (2 \cdot L_{eff})$
  - **Offset Angle (α):** $\alpha = \arcsin[ (R_1 + R_2) / (2 \cdot L_{eff}) ]$ (exact form) $\approx (R_1 + R_2) / (2 \cdot L_{eff})$ [in radians]

### 2.3 Derivation of the Classical Geometries (Loefgren A/Baerwald, Loefgren B, Stevenson)

Given the minimum recorded radius $R_{min}$ and the maximum recorded radius $R_{max}$ of the disc side, the three historical geometries solve the minimization problem with different criteria:

1. **Loefgren A (Baerwald, 1941) — Chebyshev Minimax Criterion:**
   Minimizes the maximum absolute value of the weighted error WTE(R) over the whole interval $[R_{min}, R_{max}]$. By Chebyshev's equioscillation theorem, the optimum is reached when the three absolute local maxima of |WTE(R)| (located at $R_{min}$, at the intermediate radius $R_m$ and at $R_{max}$) are exactly equal in magnitude:
   $|WTE(R_{min})| = |WTE(R_m)| = |WTE(R_{max})|$
   From this the positions of the null points are obtained:
   - $R_{hm} = (2 \cdot R_{min} \cdot R_{max}) / (R_{min} + R_{max})$
   - $R_{1,2} = (2 \cdot R_{min} \cdot R_{max}) / [ (R_{max} + R_{min}) \pm (\sqrt{2} / 2) \cdot (R_{max} - R_{min}) ]$ (+ sign for $R_1$, – sign for $R_2$; derivation in §6.2)
2. **Loefgren B (1938) — Root-Mean-Square (RMS) Error Minimization:**
   Minimizes the integral of the squared weighted error over the entire recorded surface:
   $\int [WTE(R)]^2 \, dR$ = minimum (integrated from $R_{min}$ to $R_{max}$)
   It reduces the weighted error and the distortion between the two null points by approx. one third (for most of the duration of the track), at the cost of a slightly higher error peak at the inner limit $R_{min}$ and the outer limit $R_{max}$ compared with Baerwald.
3. **Stevenson (J.K. Stevenson, 1966) [3] — Inner Groove Protection:**
   Places the first null point exactly at the minimum recorded radius ($R_1 = R_{min}$), where the linear velocity is lowest and the orchestral tutti of symphonic music are most critical, and equalizes only the two remaining peaks (the intermediate peak between $R_1$ and $R_2$ and the peak at the outer edge $R_{max}$).

### 2.4 Groove Radius Standards (IEC 60098 vs DIN 45547 vs JIS)

The numerical values of the null points depend strictly on the radial limits $R_{min}$ and $R_{max}$ assumed by the reference standard:

- **IEC 60098 (1958) / RIAA [4]:** $R_{min}$ = 60.325 mm, $R_{max}$ = 146.05 mm.
- **DIN 45547 (Germany) [5]:** $R_{min}$ = 57.50 mm, $R_{max}$ = 146.05 mm (considers discs cut very close to the label; later editions of DIN and IEC raise $R_{max}$ to 146.30 mm).
- **JIS S8502-1973 (Japan) [6]:** $R_{min}$ = 57.60 mm, $R_{max}$ = 146.50 mm.

### 2.5 Numerical Comparison Table: 9", 10" and 12" Tonearms (IEC Standard: $R_{min}$ = 60.325 mm, $R_{max}$ = 146.05 mm)

| Nominal Length and $L_{eff}$ | Geometry | Inner Null Point $R_1$ (mm) | Outer Null Point $R_2$ (mm) | Overhang O (mm) | Pivot-Spindle Distance $D_{p2s}$ (mm) | Offset Angle α (degrees) | WTE Max (°/cm) |
|---|---|---|---|---|---|---|---|
| **9-inch ($L_{eff}$ = 229 mm)** | **Loefgren A (Baerwald)** | 66.00 | 120.90 | 18.14 | 210.86 | 24.08° | 0.130 |
| **9-inch ($L_{eff}$ = 229 mm)** | **Loefgren B** | 70.29 | 116.60 | 18.65 | 210.35 | 24.08° | 0.212 |
| **9-inch ($L_{eff}$ = 229 mm)** | **Stevenson** | 60.325 | 117.42 | 16.03 | 212.97 | 22.84° | 0.158 |
| **10-inch ($L_{eff}$ = 254 mm)** | **Loefgren A (Baerwald)** | 66.00 | 120.90 | 16.23 | 237.77 | 21.59° | 0.115 |
| **10-inch ($L_{eff}$ = 254 mm)** | **Loefgren B** | 70.29 | 116.60 | 16.68 | 237.32 | 21.59° | 0.188 |
| **10-inch ($L_{eff}$ = 254 mm)** | **Stevenson** | 60.325 | 117.42 | 14.35 | 239.65 | 20.48° | 0.139 |
| **12-inch ($L_{eff}$ = 305 mm)** | **Loefgren A (Baerwald)** | 66.00 | 120.90 | 13.37 | 291.63 | 17.84° | 0.093 |
| **12-inch ($L_{eff}$ = 305 mm)** | **Loefgren B** | 70.29 | 116.60 | 13.75 | 291.25 | 17.84° | 0.152 |
| **12-inch ($L_{eff}$ = 305 mm)** | **Stevenson** | 60.325 | 117.42 | 11.84 | 293.16 | 16.94° | 0.113 |

*(Technical note on 12-inch arms such as the SME 3012 / 3012-R: increasing $L_{eff}$ from 229 mm to 305 mm reduces the maximum weighted error and the harmonic distortion due to tracking by approx. 28% (Baerwald WTE max from 0.130 to 0.093 °/cm), while also reducing the offset angle α and, consequently, the magnitude of the skating force).*

## 3. Tribology, Vector Forces and Fine Adjustments

### 3.1 Vertical Tracking Force (VTF) and Generator Centering

The VTF (Vertical Tracking Force, expressed in gram-force or millinewtons, where 1 g ≈ 9.81 mN) serves two primary functions:

1. **Maintaining mechanical contact:** It provides the normal force needed to counter the vertical and lateral accelerations imparted by the groove modulation (at the stylus tip, several hundred g are exceeded at high frequency: 10 cm/s at 10 kHz corresponds to approx. 640 g).
2. **Geometric alignment of the magnetic generator:** In MC cartridges in particular, the static preload of the VTF flexes the tie-wire (rear tensioning wire) and compresses the elastomer until the moving coil sits exactly at the symmetric center of the magnetic flux generated by the pole pieces (air gap).
    - *VTF too low:* Severe risk of mistracking (the stylus bounces against the groove walls, damaging the vinyl more than a high VTF would) and asymmetry of the magnetic field with increased second-harmonic

distortion.

- *VTF too high:* The coils operate off-axis with respect to the center of the magnetic flux, the suspension enters a region of nonlinear compression (stiffening of the elastomer) and the cartridge body risks bottoming out on the disc.

### 3.2 Vector Analysis of the Skating Force and Compensation (Anti-Skating)

Because the line of action of the dynamic friction force $F_f$ (tangent to the groove at the stylus contact point) does not pass through the arm pivot, owing to the overhang and the offset angle α, the forces undergo a vector decomposition.
Letting $F_f = \mu \cdot VTF$ be the sliding friction force between diamond and PVC:

- The longitudinal component $F_t = F_f \cdot \cos(\alpha + \theta_e)$ puts the armtube in tension toward the pivot.
- The normal component $F_{skating}$ generates a torque that pushes the arm toward the center of the disc:

$$\mathbf{F_{skating} = F_f \cdot \sin(\alpha + \theta_e) = \mu \cdot VTF \cdot \sin(\alpha + \theta_e)}$$

Physical variables that prevent perfect static compensation:

- The dynamic friction coefficient μ (typically between 0.22 and 0.45) is not constant: it increases as the groove modulation velocity increases (a high-level musical passage generates a skating force up to 30–40% higher than an unmodulated groove) and varies significantly with the stylus profile and the cleanliness of the vinyl.
- The angle $(\alpha + \theta_e)$ varies along the disc radius, showing a minimum at the intermediate radius and two maxima at the outer and inner edges.
- *Instrumental adjustment:* Using a smooth disc (without grooves) overestimates or falsifies the equilibrium point because the contact area of the tip rests on the bottom instead of on the two walls at 45°; correct calibration is performed by observing on an oscilloscope the symmetric onset of clipping (mistracking) on the L and R channels with high-modulation test tracks (e.g., 300 Hz or 315 Hz at +12 dB / +15 dB, corresponding to 50–80 μm of lateral amplitude).

### 3.3 Diamond Geometry, VTA (Vertical Tracking Angle) and SRA (Stylus Rake Angle)

- **VTA (Vertical Tracking Angle):** The angle formed by the line joining the cantilever pivot to the stylus tip relative to the disc surface, projected onto the lateral vertical plane. The modern IEC/RIAA standard specifies a nominal cutting angle of 20° (±5°).
- **SRA (Stylus Rake Angle):** The angle formed by the vertical axis of the diamond contact profile relative to the perpendicular to the disc plane. Because, when cutting the lacquer master, the cutting stylus (heated and with suction) is tilted slightly forward to facilitate the removal of the chip, the effective cutting angle is typically between **92° and 93°** (2°–3° beyond vertical).
- **Geometric sensitivity:** A change of 1 mm in the height of the arm base (VTA pillar) on a 9-inch arm (229 mm) produces an angular change of only:

$$\mathbf{\Delta\theta = \arctan(1 / 229) \approx 0.25^\circ}$$ ***(a quarter of a degree)***

To obtain a 1° change in SRA on a 9" arm, approx. 4 mm of vertical travel of the tower is needed (and approx. 5.3 mm on a 12" arm).

### 3.4 Comparison Table of Stylus Profiles

| Stylus Profile | Minor Radius r (μm) × Major Radius R (μm) | Typical Contact Area (μm²) | Sensitivity to VTA/SRA and Azimuth | Tracking and Wear Characteristics |
|---|---|---|---|---|
| **Spherical / Conical** (e.g., Denon DL-103, Ortofon SPU Classic) | 15 – 18 μm (single radius, 25 μm for mono/historical LPs) | ~18 – 22 | Very low (the contact profile does not change with VTA and Azimuth). | "Pinch effect" at high frequencies; excellent immunity to surface defects; lifetime ~400–600 hours. |
| **Elliptical (Biradial)** | 8 × 18 μm (or 7 × 18 μm) | ~12 – 15 | Moderate. | Better high-frequency response in the inner grooves than conical; higher specific pressure; lifetime ~500–700 hours. |
| **Hyper-Elliptical / Shibata / Fine Line** | 6 × 40 μm ÷ 6 × 75 μm | ~25 – 35 | High (requires accurate SRA and Azimuth alignment). | Large vertical footprint that distributes the VTF and reduces groove wear; developed for CD-4 quadraphonic (up to 45 kHz). |
| **MicroRidge / MicroLine / Replicant 100 / Gyger S** | 2 × 75 μm ÷ 5 × 100 μm | ~35 – 45 | Extreme (ideal SRA tolerance within ±0.5° of 92°). | Minor radius of 2–3 μm that matches the cutting stylus profile; minimal tracking distortion up to the end of the disc; lifetime ~1000+ hours owing to the constant micro-ridge edge. |

### 3.5 Azimuth, Crosstalk and Phase Balance

In the Westrex 45°/45° stereo system, the left channel (L) is cut on the inner groove wall and the right channel (R) on the outer wall, orthogonal to each other.

- An Azimuth error (axial rotation of the cartridge seen from the front) alters the orthogonality between the sensitivity axes of the L/R generators and the groove walls, degrading channel separation (Crosstalk) and introducing a relative phase shift at high frequency between L and R.
- Because the mechanical mounting of the diamond on the cantilever and of the coils on the core has manufacturing tolerances of ±1° ÷ 2°, leveling the top surface of the headshell perfectly does not guarantee correct electrical Azimuth.
- **Instrumental calibration procedure:** A 1 kHz test track cut on the L channel only is played and the residual signal induced on the R channel (L→R crosstalk) is measured in dBV (or mV RMS); the operation is then repeated with the R-only track (R→L crosstalk). The optimal Azimuth is obtained when the two crosstalk attenuations are equal (e.g., -30 dB on both channels) with minimum relative phase shift.

## 4. Structural Resonances, Flexural Modes and Material Damping

Besides the fundamental rigid-body resonance $f_0$ (8–12 Hz), the armtube and the headshell carrier are subject to natural modes of elastic vibration (flexural and torsional) well within the audio band (typically between 150 Hz and 2500 Hz), excited by the mechanical energy that the stylus does not convert into an electrical signal but transmits through the cartridge body.

- **Flexural frequency equation of a beam (Euler-Bernoulli):**
  The first natural bending frequency of a tubular armtube is proportional to the speed of sound propagation in the material and to the radius of gyration of the cross-section:

$$f_{flex} \propto (d_{ext} / L^2) \cdot \sqrt{(E / \rho)}$$

Where:

- **E:** Young's modulus (longitudinal elasticity).
- **ρ:** Volumetric density of the material.

- **$\sqrt{(E / \rho)}$:** Specific speed of acoustic propagation in the medium.
- **$d_{ext}$:** Outer diameter of the tube (for equal mass and with a thin wall, the flexural stiffness grows with the square of the diameter and the flexural frequency grows in proportion to the diameter).
- **Acoustic Properties of Materials for Armtubes and Headshells:**
  - **Aluminum (e.g., Alloy 6061/7075):** $\sqrt{(E / \rho)} \approx 5100$ m/s; low internal damping (loss factor η). Often surface-treated (hard anodizing) or internally filled with polyurethane foam/balsa wood to lower the Q of the tubular resonances.
  - **Magnesium (e.g., SME Series V monoblock casting):** $\sqrt{(E / \rho)} \approx 5000$ m/s; very low density (1.74 g/cm³) and very high internal damping coefficient (η ~ 10 times that of aluminum).
  - **Titanium / Stainless Steel (e.g., Fidelity Research FR-64S):** High density and very high structural stiffness; shifts energy reflections by means of the mechanical impedance mismatch between the cartridge shell and the heavy armtube.
  - **Carbon Fiber (CFRP):** $\sqrt{(E / \rho)} \approx 9000 – 11\,000$ m/s; shifts the flexural modes toward very high frequencies, but requires damping resins or hybrid layups to avoid high-Q resonances between 800 Hz and 2 kHz.
  - **Dense Woods (Ebony, Cocobolo, Panzerholz for headshells and spacers):** Anisotropic acoustic velocity and high internal viscous damping of the cellular fibers; excellent as a mechanical interface (spacers) between the cartridge body and the metal headshell to interrupt standing waves.

## 5. Advanced Electrical Interfacing: Cartridge, Wiring, SUT and Phono Stage

### 5.1 Thévenin Equivalent Circuit and Complex Transfer Function

From an electrical engineering standpoint, any magnetodynamic cartridge (MM, MI, MC) is a reciprocal electromechanical transducer operating according to the Faraday-Neumann-Lenz law ($V_{gen} = -N \cdot d\Phi/dt$). Because it is a velocity-sensitive generator, the open-circuit electromotive force $V_{gen}(\omega)$ rises linearly with frequency (+6 dB/octave, or +20 dB/decade) for a constant groove modulation amplitude.
The Thévenin/Norton equivalent model places the ideal generator $V_{gen}$ in series with the internal coil impedance $Z_c(s)$:

- **$R_c$:** Ohmic direct-current (DC) resistance of the copper or silver windings.
- **$L_c(\omega)$:** Series inductance of the coil (frequency-dependent because of eddy-current (Foucault) losses in the magnetic core, especially in MM/MI cartridges with laminated pole pieces).
- **$R_{loss}(\omega)$:** Equivalent parallel resistance representing the iron losses (magnetic hysteresis and eddy currents) at high frequency.

This generator drives a passive two-port network (tonearm wiring + external phono cable) terminated by the input impedance of the active phono stage (or of the step-up transformer):

- **$C_{tot}$:** Total parallel capacitance seen from the cartridge terminals:
  $C_{tot} = C_{pins}$ (inter-electrode capacitance of the cartridge/clip pins, ~3–5 pF) + $C_{arm}$ (Litz wires inside the tonearm, ~15–35 pF) + $C_{cable}$ (external phono cable, typically 45–120 pF/m) + $C_{in}$ (discrete input capacitance of the preamplifier) + $C_{Miller}$ (dynamic Miller capacitance of the active input stage).
- **$R_{in}$:** Input termination resistance of the phono stage (or the secondary resistance reflected to the primary in the case of transformer coupling).

The voltage transfer function $H(s) = V_{out}(s) / V_{gen}(s)$ (with $s = j\omega$) forms a second-order resonant low-pass filter:

$$\mathbf{H(s) = [\ R_{in} / (R_c + R_{in})\ ] / [\ s^2 \cdot L_c \cdot C_{tot} \cdot (R_{in} / (R_c + R_{in})) + s \cdot (\ (L_c + R_c \cdot R_{in} \cdot C_{tot}) / (R_c + R_{in})\ ) + 1\ ]}$$

Assuming the standard voltage-transfer condition ($R_{in} >> R_c$), the canonical parameters of the complex-conjugate pole are:

- **Undamped natural frequency ($f_e$):**
  $f_e = 1 / [ 2\pi \cdot \sqrt{(L_c \cdot C_{tot})} ]$
- **Damping ratio ($\zeta$) and electrical quality factor ($Q_e$):**
  $\zeta = (1 / 2) \cdot [ R_c \cdot \sqrt{(C_{tot} / L_c)} + (1 / R_{in}) \cdot \sqrt{(L_c / C_{tot})} ]$
  $Q_e = 1 / (2 \cdot \zeta) = 1 / [ R_c \cdot \sqrt{(C_{tot} / L_c)} + (1 / R_{in}) \cdot \sqrt{(L_c / C_{tot})} ]$

To obtain a maximally flat response (Butterworth alignment, where $Q_e = 1/\sqrt{2} \approx 0.707$, with no passband overshoot and a monotonic roll-off), the relationship between load resistance $R_{in}$, inductance $L_c$ and total capacitance $C_{tot}$ must satisfy (neglecting $R_c$ relative to $R_{in}$):

**$R_{in}(optimal_Butterworth) \approx \sqrt{(L_c / (2 \cdot C_{tot}))}$**

### 5.2 Electrical Dynamics of MM (Moving Magnet) and MI (Moving Iron) Cartridges

- **Typical physical parameters:**
  - Nominal output voltage (1 kHz, 5 cm/s RMS): 2.5 mV – 6.0 mV.
  - Internal inductance ($L_c$): 350 mH – 800 mH (e.g., Shure V15 Type III: $L_c$ = 500 mH, $R_c$ = 1350 Ω; Nagaoka MP-700 / MP series: low-mass MI, inductance not published by Nagaoka, est. ~450–550 mH).
- **Conjugate electromechanical equalization:**
  In MM cartridges, the effective tip mass (ETM, typically 0.3 – 0.6 mg) introduces a mechanical resonance of the cantilever on the vinyl (due to the local elastic compliance of the PVC groove, Hertz law) at around 14–18 kHz, followed by a severe mechanical roll-off. Designers choose $L_c$ and specify a particular $C_{tot}$ (e.g., 100–200 pF for Audio-Technica, 250–300 pF for Ortofon, 400–500 pF for Shure V15 Type III) so that the electrical pole $f_e$ supports precisely the mechanical droop before the final cutoff above 20 kHz.
- **Deviations from the optimal load ($R_{in}$ and $C_{tot}$):**
  - **Excess capacitance ($C_{tot} > C_{target}$):** Lowers $f_e$ to 9–12 kHz and at the same time reduces damping (because the term $(1/R_{in})\cdot\sqrt{(L_c/C_{tot})}$ decreases, raising $Q_e$). The result is a sharp peak of +3 to +6 dB around 10 kHz followed by an attenuation of -12 dB/octave that wipes out the first upper octave (12–20 kHz).
  - **$R_{in}$ variation beyond the standard 47 kΩ (e.g., 33 kΩ or 68–100 kΩ):** Reducing $R_{in}$ to 32–38 kΩ directly lowers $Q_e$, damping the resonance peaks of particularly bright MM cartridges without shifting the center frequency $f_e$; conversely, raising $R_{in}$ to 68–100 kΩ accentuates the peak at $f_e$.
- **Effect of Miller Capacitance in Tube (Triode) Phono Stages:**
  When the first stage of the phono preamplifier uses a high-gain triode (e.g., 12AX7 / ECC83 in classic circuits such as the McIntosh C22 or Conrad-Johnson PV12), the dynamic input capacitance seen by the cartridge is not just the geometric grid-cathode capacitance ($C_{gk} \approx 1.6$ pF) but includes the grid-plate capacitance ($C_{ga} \approx 1.7$ pF) multiplied by the voltage gain of the inverting stage (Miller effect):
  $C_{Miller} = C_{gk} + C_{ga} \cdot (1 + A_v)$
  With a first-stage gain $A_v \approx 35–45$ (approx. 31–33 dB), the tube alone presents a dynamic capacitance of:
  $C_{Miller} \approx 1.6$ pF + 1.7 pF · (1 + 40) ≈ **71.3 pF**
  Adding to these 71 pF the capacitance of the input capacitors per CE/FCC regulations and of the turntable cable, the 200–250 pF threshold is easily exceeded. This makes very-low-capacitance-per-length phono cables essential (e.g., Mogami 2964 at 65 pF/m or Van den Hul D-502 Hybrid at 75 pF/m) so as not to overload MM and MI cartridges that require low total loads (e.g., Nagaoka MP: 100 pF; Audio-Technica: 100–200 pF).

### 5.3 Electrical Dynamics of MC (Low-Output Moving Coil) Cartridges

- **Typical physical parameters:**
  - Nominal output voltage (1 kHz, 5 cm/s RMS): 0.15 mV – 0.60 mV.
  - Internal inductance ($L_c$): 1.5 µH – 35 µH.

- Internal DC resistance ($R_c$): 1.5 Ω – 40 Ω (e.g., Ortofon SPU Classic ~2 Ω, Fidelity Research FR-7 ~2 Ω, Koetsu Onyx ~5 Ω, Kiseki Purple Heart ~42 Ω, Hana SL Mono 30 Ω, MkII 23 Ω).

- **Radio-Frequency (RF) Behavior and Zobel Network (RC Snubber):**
  With $L_c$ = 8 μH and $C_{tot}$ = 150 pF, the electrical resonance frequency falls at:
  $f_e = 1 / [ 2\pi \cdot \sqrt{(8 \cdot 10^{-6}\ H \cdot 150 \cdot 10^{-12}\ F)} ] \approx$ **4.59 MHz**
  The quality factor is $Q_e = 1 / [ R_c \cdot \sqrt{(C_{tot} / L_c)} + (1 / R_{in}) \cdot \sqrt{(L_c / C_{tot})} ]$. With a high-impedance input (47 kΩ), damping relies almost entirely on $R_c$, which is only a few ohms: with $R_c$ = 5 Ω, $Q_e \approx 38$ (a peak of more than +30 dB at RF). With a 100 Ω load, the second term dominates instead and $Q_e$ drops to approx. 0.4: the RF resonance is overdamped. This is the physical reason why a low resistive load has an effect on MC cartridges even though it does not touch the audio band.
- **Practical consequences:** Even though the 4.5 MHz pole does not alter the magnitude of the frequency response at 20 kHz, with a high-impedance load the LC circuit acts as a tank circuit tuned to the short/medium waves and amplifies the impulsive noise of vinyl "clicks/pops" (which have sub-microsecond rise times), driving the first active stage of the phono preamp into slew-rate saturation or intermodulation (AM rectification on the parasitic input diodes of JFETs/BJTs).
  - **Zobel cell calculation (RF critical damping):** To cancel the RF peak, many state-of-the-art MC preamplifiers insert at the input a series RC ($R_z + C_z$) calculated to critically damp $L_c$:
    $R_z \approx \sqrt{(L_c / C_{tot})}$ with $C_z \geq (3 \text{ to } 5) \cdot C_{tot}$

**Voltage Divider, Phase and Lenz Electrodynamic Damping:**
In the audio band (20 Hz – 20 kHz) the inductive reactance $X_L = 2\pi \cdot f \cdot L_c$ is below 1–3 Ω. The signal transfer to an active stage with input resistance $R_{in}$ is governed by the resistive divider law:
Insertion loss (dB) = $20 \cdot \log_{10} [ R_{in} / (R_c + R_{in}) ]$

- - **If $R_{in} = 10 \cdot R_c$:** Loss = -0.83 dB (90.9% of the voltage transferred).
  - **If $R_{in} = 5 \cdot R_c$:** Loss = -1.58 dB (83.3% of the voltage transferred).
  - **If $R_{in} = R_c$ (maximum power transfer matching):** Loss = -6.02 dB (50% of the voltage transferred).

**Physical mechanism of electromagnetic damping:**
When the cantilever oscillates with velocity v(t), the current $I(t) = V_{gen}(t) / (R_c + R_{in})$ flowing in the coil immersed in the radial magnetic field B generates a mechanical counter-electromotive force (Lorentz/Lenz force):
$F_{em}(t) = (B \cdot l_{wire}) \cdot I(t) = [ (B \cdot l_{wire})^2 / (R_c + R_{in}) ] \cdot v(t)$
The term $R_{em} = (B \cdot l_{wire})^2 / (R_c + R_{in})$ has exactly the physical dimensions of a **viscous mechanical damper (N·s/m)** that adds directly in parallel to the mechanical resistance $R_m$ of the elastomer damper:
$R_m(\text{total}) = R_m(\text{elastomer}) + [ (B \cdot l_{wire})^2 / (R_c + R_{in}) ]$

1. In MC cartridges with very powerful magnets (solid Alnico or neodymium with a narrow gap, such as the FR-7, SPU or Koetsu) and coils wound on a ferromagnetic core (which multiplies B), the product $(B \cdot l_{wire})^2$ is large: terminating the cartridge in a low resistive load (e.g., $R_{in} = 2 \cdot R_c$ to $5 \cdot R_c$) significantly increases the total mechanical damping, restraining the high-frequency cantilever resonance (25–40 kHz) and giving greater focus and tonal stability.
2. In MC cartridges with air-core coils (low inductance and low BI factor), the Lenz force is negligible and the load $R_{in}$ acts almost exclusively on the damping of RF transients.

### 5.4 In-Depth Analysis of Step-Up Transformers (SUT)

The step-up transformer is the optimal electromagnetic interface for coupling low-impedance MC cartridges (1.5 Ω – 40 Ω) to tube MM phono stages with high input impedance (47 kΩ), providing galvanic isolation, common-mode noise rejection and a thermal noise figure close to the theoretical physical limit (since copper windings generate no shot or 1/f flicker noise).

### *Non-Ideal Circuit Model of the Audio Transformer*

A real transformer with turns ratio $N = N_2 / N_1$ presents four fundamental parasitic elements that determine its bandwidth and transient response:

- **1. $R_p$ and $R_s$:** Direct-current (DC) resistances of the primary and secondary windings. The effective impedance seen from the secondary includes the reflected copper losses: $R_{cu}(sec) = R_s + N^2 \cdot R_p$.
- **2. $L_p$ (Primary magnetizing inductance):** Determines the low-frequency high-pass pole (-3 dB):
  $f_{low}$ (-3 dB) = $(R_c + R_p) / (2\pi \cdot L_p)$
  *Example:* To ensure an extended response down to 5 Hz (needed to avoid introducing phase rotation at 20–30 Hz) with a cartridge of $R_c$ = 23 Ω (or 40 Ω), the primary inductance $L_p$ must be at least:
  $L_p \geq 25\ \Omega / (2\pi \cdot 5\ Hz) \approx$ **0.80 Henry** (ideally > 2–5 H using cores with very high initial permeability $\mu_i > 50\,000$ such as 80% Ni Permalloy / Mu-Metal or nanocrystalline/amorphous alloys).
  For a 2 Ω SPU or FR-7, a primary inductance of 0.15 – 0.30 H is sufficient instead, allowing fewer primary turns with heavier-gauge wire.
- **3. $L_{leak}$ (Leakage inductance, referred to the secondary):** Represents the magnetic flux that does not link both windings. It is reduced by using interleaved (interleaved/bifilar) windings.
- **4. $C_w$ (Distributed capacitance of the secondary winding):** Added to the capacitance of the output cable between SUT and MM preamp ($C_{out}$) and to the input capacitance of the MM preamp ($C_{MM} + C_{Miller}$), it forms the total secondary capacitance $C_{sec} = C_w + C_{out} + C_{in}(MM)$.

### *SUT High-Frequency Resonance and Secondary Zobel Network Calculation*

At the transformer secondary, the leakage inductance $L_{leak}$ (added to the cartridge inductance multiplied by $N^2$, i.e., $N^2 \cdot L_c$) resonates in series/parallel with the total secondary capacitance $C_{sec}$ at a critical ultrasonic frequency (typically between 18 kHz and 60 kHz):

$$\mathbf{f_{res}(SUT) = 1 / [\ 2\pi \cdot \sqrt{(\ L_{leak}(sec) \cdot C_{sec}\ )}\ ]}$$

- **Effect of a high turns ratio ($N^2$):** Because impedances scale with the square of the turns ratio ($N^2$), a transformer with N = 20 (+26 dB) or N = 30 (+29.5 dB) sees the cartridge internal resistance multiplied by 400 or 900 ($R_{c_}sec = N^2 \cdot R_c$), and the secondary capacitance reflected to the primary multiplied by 400 or 900:
  $C_{reflected}(primary) = N^2 \cdot C_{sec}$
  *(Example: 200 pF on the secondary of a 1:30 SUT is equivalent to as much as 200 pF × 900 = 180 000 pF =* **180 nF** seen directly by the cartridge coil!).
- **Square-wave ringing and Zobel network:** If the standard 47 kΩ secondary load is too high relative to the characteristic impedance of the parasitic resonance $Z_0 = \sqrt{(L_{leak} / C_{sec})}$, the transformer shows severe overshoot and ultrasonic ringing. To obtain critical damping:
  - **1. Secondary Resistive Load ($R_{load}$):** To lower the impedance seen by the cartridge to the target value $R_{target}$ (with $R_{target} < 47\,000 / N^2$), a secondary resistor $R_{aux}$ is connected in parallel with the SUT output terminals, calculated as:
    $R_{eff}(secondary) = R_{target} \cdot N^2$
    $R_{aux} = (47\,000 \cdot R_{eff}) / (47\,000 - R_{eff})$
  - **2. Zobel RC Network (Secondary Snubber):** To selectively damp the ultrasonic peak at $f_{res}(SUT)$ without loading the cartridge in the audio band, a resistor $R_z$ in series with a capacitor $C_z$ is connected in parallel with the secondary:
    $R_z \approx \sqrt{(L_{leak} / C_{sec})}$
    $C_z \approx (2 \text{ to } 4) \cdot C_{sec}$

## 5.5 Electrical Noise, Signal-to-Noise Ratio (SNR) and Choice of Active Topology

The insurmountable physical limit of any phono preamplification system is the **Johnson-Nyquist thermal noise** generated by the real resistance of the circuit at absolute temperature T (at 20 °C = 293 K):

$$V_n(\text{thermal}) = \sqrt{( 4 \cdot k_B \cdot T \cdot R \cdot \Delta f )}$$

Where $k_B = 1.38 \times 10^{-23}$ J/K is the Boltzmann constant and $\Delta f = 20\,000$ Hz is the audio bandwidth. At 20 °C, a 1 Ω resistance generates a noise spectral density of **0.127 nV/√Hz** (i.e., ~18 nV RMS over 20 kHz of unweighted bandwidth).
Every active device (JFET, BJT, thermionic tube, op-amp) is characterized by two equivalent input noise generators:

- **$e_n$ (nV/√Hz):** Series noise voltage density.
- **$i_n$ (pA/√Hz):** Parallel noise current density (which, flowing through the cartridge impedance $Z_c(\omega)$, generates an additional noise voltage $V_{ni} = i_n \cdot |Z_c(\omega)|$).

The total input-referred noise voltage (before RIAA de-emphasis) is:

$$E_n(\text{tot}) = \sqrt{[ 4 \cdot k_B \cdot T \cdot R_c + e_n^2 + (i_n \cdot |R_c + j\omega L_c|)^2 ]}$$

From this fundamental equation follows the optimal pairing between cartridge type and electronic architecture:

- **1. Tube Triode Stages (e.g., 12AX7, 6DJ8/ECC88, 6922, E88CC):**
  - They have almost zero grid noise current ($i_n \rightarrow$ fA/√Hz), but a relatively high noise voltage density ($e_n \approx 2 – 12$ nV/√Hz: approx. 2 for 6DJ8/ECC88, 5–6 for 12AX7).
  - They are **excellent for MM cartridges** (where the source impedance at 10 kHz exceeds 30 kΩ and the $i_n \cdot |Z_c|$ term dominates, making BJTs noisy), but are unsuitable for driving low-output MC cartridges (0.2 mV) directly without a step-up transformer (SUT) in between, since the SUT raises the signal by a factor of N, bringing it above the tube's $e_n$ noise floor.
- **2. Discrete JFET Stages (e.g., 2SK170, 2SK369, LSK389 in parallel):**
  - They exhibit very low $e_n$ (~0.8 – 1.2 nV/√Hz per single device, reduced by √M by paralleling M JFETs) and negligible noise current $i_n$ (~0.01 pA/√Hz).
  - They are the most versatile solid-state architecture for both MM and medium-impedance MC (10 – 40 Ω), with the only caveat of managing the high gate-source capacitance $C_{iss}$ (30–60 pF for a single 2SK170) through a cascode configuration to cancel the Miller effect.
- **3. Bipolar Junction Transistor (BJT) Stages (e.g., 2SB737, MAT02/03, SSM2210, large-base-area BJTs):**
  - They offer the lowest noise voltage available ($e_n \approx 0.4 – 0.7$ nV/√Hz) thanks to a very low base spreading resistance $r_{bb}'$, but present a significant noise current $i_n$ (~1.5 – 3 pA/√Hz).
  - They are **unbeatable for MC cartridges with very low internal impedance ($R_c$ = 1.5 – 10 Ω)**, where the $i_n \cdot R_c$ term is irrelevant, while they are noisy with high-inductance MM cartridges.

### 5.6 Wiring Architecture: Balanced (XLR) vs. Unbalanced (RCA) Connection

A phono cartridge is by its physical nature a **natively balanced, floating source (floating balanced source)**: the four output pins (L+, L-, R+, R-) are the isolated ends of two independent windings, with no ground reference (except for a removable metal tab on the RG or LG pin in some MM cartridges).

1. **Unbalanced Connection (RCA / Coaxial):**
   The cold pole (L- / R-) is connected to the shield braid or to the return conductor referenced to the preamplifier chassis. Any stray current or electromagnetic disturbance induced on the return conductor adds directly in series with the useful signal (IR voltage drop along the ground). To minimize this defect, cables in a ***Pseudo-Balanced (Semi-Balanced / Directional Shield)*** configuration are used: an internal twisted pair carries L+ and L-, while the copper shield braid is connected to ground only at the turntable/preamplifier end, acting as a Faraday cage without carrying signal current.
2. **True Balanced Connection (True Balanced on XLR or DIN-5 → Dual XLR):**
   The coil poles L+ and L- travel on two identical symmetrical conductors to a differential input (or to the ends of

the floating primary winding of a SUT), while the shield is connected to Pin 1 (Chassis Ground), isolated from the signal.

- **Measurable advantages:** Alternating magnetic fields at 50 Hz (power transformers, high-torque synchronous motors such as those of classic idler-wheel turntables) and RF interference couple identically onto both conductors (common mode) and are canceled by the common-mode rejection (CMRR > 60–80 dB) of the differential stage or of the step-up transformer, lowering the hum floor by 20–30 dB.

### 5.7 RIAA De-Emphasis and Overload Margin

The standard RIAA equalization curve (1954) [7] is defined by three time constants that determine two poles and one zero in the preamplifier de-emphasis network:

1. **$\tau_1$ = 3180 µs** → Bass corner frequency (pole): $f_1 = 1 / (2\pi \cdot 3180 \cdot 10^{-6})$ = **50.05 Hz** (+19.3 dB at 20 Hz relative to 1 kHz).
2. **$\tau_2$ = 318 µs** → Central transition frequency (zero): $f_2 = 1 / (2\pi \cdot 318 \cdot 10^{-6})$ = **500.5 Hz** (0 dB at 1 kHz).
3. **$\tau_3$ = 75 µs** → Treble corner frequency (pole): $f_3 = 1 / (2\pi \cdot 75 \cdot 10^{-6})$ = **2122 Hz** (-19.6 dB at 20 kHz relative to 1 kHz).
   *(Note on the Neumann time constant $\tau_4$ = 3.18 µs / 50.05 kHz: introduced in some phono preamps to compensate for the supposed ultrasonic rolloff of Neumann cutting lathes, it is in fact not part of the recording standard and artificially boosts the extreme treble by +0.17 dB at 10 kHz and +0.64 dB at 20 kHz).*

#### *The Critical Problem of Overload Margin at High Frequency*

Because the record is cut with a **pre-emphasis of +20 dB at 20 kHz**, the peak groove velocity in high-frequency transients (cymbals, sibilant consonants, brass, or even a simple surface scratch/tick) reaches values of up to 40–60 cm/s at 10–20 kHz (i.e., **10 times (+20 dB)** the nominal reference level of 5 cm/s at 1 kHz).

1. **Passive RIAA (Split or Full Passive):** The first gain stage amplifies the "flat" signal before the passive RIAA filter. If the first stage has too much gain or a low supply voltage, a high-frequency transient or a vinyl click (amplified by +20 dB by the cutting process before it even meets the RIAA attenuation) clips the first active stage, turning an inaudible micro-impulse lasting a few microseconds into a wide, unpleasant "snap" in the audio band.
2. **Active RIAA in Negative Feedback (NFB):** The amount of negative feedback increases by 20 dB going from 1 kHz to 20 kHz, proportionally increasing the input overload margin at high frequencies, but requires the first stage to have a very high slew rate and an unconditional phase stability margin when the feedback impedance collapses toward zero in the ultrasonic band.

### 5.8 Technical Reference Table: Electrical Interfacing Calculations for Classic and Modern Cartridges

| Cartridge Model | Type | Output Voltage (1 kHz, 5 cm/s) | Internal $R_c$ (Ω) | Internal $L_c$ | Optimal Active Load ($R_{in}$ / $C_{tot}$) | Ideal SUT Coupling (Ratio N and $R_{ref}$ on 47 kΩ) | Recommended Total Phono Gain (for ~500 mV out) |
|---|---|---|---|---|---|---|---|
| **Ortofon SPU Classic GE / Mono** | Low-Impedance MC | 0.20 mV | 2.0 Ω | ~2.5 µH | $R_{in}$: 20 Ω – 50 Ω (or Current-Mode) | 1:30 (+29.5 dB) → $R_{ref}$ = 52 Ω (or 1:40 → 29 Ω) | 66 – 70 dB |
| **Fidelity Research FR-7** | Low-Impedance MC (push-pull, two magnets) | 0.20 mV | 2.0 Ω | ~2.0 µH | $R_{in}$: 20 Ω – 40 Ω | 1:30 (+29.5 dB) → $R_{ref}$ = 52 Ω | 66 – 70 dB |
| **Koetsu Onyx / Rosewood** | Low-Impedance MC | 0.30 – 0.40 mV | 5.0 Ω | ~6.0 µH | $R_{in}$: 50 Ω – 100 Ω | 1:20 (+26 dB) → $R_{ref}$ = 117.5 Ω | 62 – 66 dB |
| **Hana SL / SL Mono** | Medium-Impedance MC (Alnico) | 0.50 mV (MkII: 0.40 mV) | 30 Ω (SL Mono first series) / 23 Ω (SL Mono MkII) | ~28 µH | $R_{in}$: ≥ 400 Ω (MkII: ≥ 230 Ω) | 1:10 (+20 dB) → $R_{ref}$ = 470 Ω (or 1:12 → 326 Ω) | 60 – 63 dB |
| **Kiseki Purple Heart NS** | Medium-Impedance MC | 0.48 mV | 42.0 Ω | ~38 µH | $R_{in}$: 400 Ω – 800 Ω | 1:10 (+20 dB) → $R_{ref}$ = 470 Ω | 60 – 63 dB |
| **Denon DL-103** | Historic Broadcast MC | 0.30 mV | 40.0 Ω | ~35 µH | $R_{in}$: 400 Ω – 1000 Ω | 1:10 (+20 dB) → $R_{ref}$ = 470 Ω (or 1:13 → 278 Ω) | 62 – 65 dB |
| **Shure V15 Type III** | Classic MM (Laminated) | 3.50 mV | 1350 Ω | 500 mH | $R_{in}$ = 47 kΩ / $C_{tot}$ = 400 – 500 pF | Not applicable (Direct MM input) | 40 – 43 dB |
| **Nagaoka MP-700 / MP-500** | MI (Permalloy / Samarium-Cobalt) | 4.00 mV (MP-700) | n/a (not published) | n/a (est. ~500 mH) | $R_{in}$ = 47 kΩ / $C_{tot}$ = 100 pF (Nagaoka data) | Not applicable (Direct MM input) | 40 – 42 dB |

## 6. Mathematical Appendix: Complete Analytic Derivation of the Alignment Geometries

### 6.1 Exact Geometric Model and First-Order Linearization

Consider the triangle formed by the spindle $O_p$ (Spindle), the tonearm pivot P (Pivot) and the stylus tip S (Stylus) located at radial distance R from $O_p$.
Let:

- **L:** Effective length of the tonearm ($L_{eff}$ = distance PS).
- **D:** Distance between pivot and spindle ($D_{p2s}$ = distance $PO_p$).
- **O:** Linear overhang (O = L - D).
- **α:** Offset angle of the cartridge with respect to the longitudinal axis PS.

Applying the law of cosines to the triangle $O_p$-P-S, the angle γ formed by the segment R (groove radius) and the segment L (tonearm axis) is:

$$\cos(\gamma) = (R^2 + L^2 - D^2) / (2 \cdot R \cdot L)$$

Since the tangent to the groove is orthogonal to the radius R, the angle between the longitudinal axis of the tonearm L and the groove tangent is (90° - γ), whose sine coincides with cos(γ):

$$\sin(\phi(R)) = (R^2 + L^2 - D^2) / (2 \cdot R \cdot L)$$

Introducing the offset angle α of the cartridge body, the absolute angular tracking error $\theta_e(R)$ is:

$$\theta_e(R) = \arcsin[ (R^2 + L^2 - D^2) / (2 \cdot R \cdot L) ] - \alpha$$

Defining the constant linear geometric parameter $K = (L^2 - D^2) / 2 = L \cdot O - O^2 / 2$, and carrying out a first-order Taylor series expansion for small angles ($\arcsin(x) \approx x$ in radians), the radius-weighted tracking error $WTE(R) = \theta_e(R) / R$ takes the rational algebraic form:

$$\mathbf{WTE(R) = [\ 1 / (2 \cdot L)\ ] - (\alpha / R) + [\ K / (L \cdot R^2)\ ]}$$

Canonical Loefgren/Baerwald change of variable:
Setting the inverse radius variable $u = 1 / R$ (groove curvature, ranging from $u_{min} = 1 / R_{max}$ at the outer edge to $u_{max} = 1 / R_{min}$ at the inner groove), the function WTE(u) becomes a convex parabola in the curvature domain u:

$$\mathbf{W(u) = (K / L) \cdot u^2 - \alpha \cdot u + [\ 1 / (2 \cdot L)\ ]}$$

The two roots of the parabola $W(u) = 0$ correspond to the null curvatures $u_1 = 1 / R_1$ and $u_2 = 1 / R_2$. By the relations between the roots and the coefficients of a quadratic polynomial:

- $u_1 + u_2 = (R_1 + R_2) / (R_1 \cdot R_2) = \alpha \cdot L / K$
- $u_1 \cdot u_2 = 1 / (R_1 \cdot R_2) = 1 / (2 \cdot K) \implies \mathbf{K = (R_1 \cdot R_2) / 2}$

From these follow the two universal laws that relate any pair of Null Points ($R_1$, $R_2$) to the mechanical geometry of the tonearm:

1. **Pivot-to-Spindle Distance:** $D = \sqrt{(L^2 - R_1 \cdot R_2)} \implies$ **Overhang: $O = L - \sqrt{(L^2 - R_1 \cdot R_2)}$**
2. **Offset Angle:**

   > $$\mathbf{\alpha = \arcsin[\ (R_1 + R_2) / (2 \cdot L)\ ]}$$

   (exact relation, with no approximations: the sine appears, not the tangent).

### 6.2 Analytic Solution of Loefgren A (Baerwald) — Chebyshev Polynomial $T_2(x)$

The Loefgren A / Baerwald criterion imposes the minimization of the infinity norm (absolute maximum peak) of W(u) over the interval $[u_{min}, u_{max}]$.
According to Chebyshev's theorem, the monic polynomial of degree 2 that exhibits the minimum maximum deviation from the zero axis over the normalized interval [-1, +1] is the Chebyshev polynomial of the first kind $T_2(x)$ divided by 2:

$$\mathbf{P_2(x) = (1 / 2) \cdot T_2(x) = x^2 - 1/2}$$

Its three extrema of equal magnitude ($|P_2| = 1/2$) are located at $x = -1$, $x = 0$, $x = +1$, and its two zeros (Null Points) fall at:

$$\mathbf{x_{1,2} = \pm \sqrt{(1 / 2)} = \pm (\sqrt{2} / 2) \approx \pm 0.7071068}$$

Mapping the physical curvature interval $[u_{min}, u_{max}]$ linearly onto the normalized interval [-1, +1] through the affine transformation:

$$\mathbf{u(x) = u_m + \Delta u \cdot x}$$

Where:

- **$u_m$ (mean curvature):** $u_m = (u_{max} + u_{min}) / 2 = (R_{max} + R_{min}) / (2 \cdot R_{min} \cdot R_{max}) = 1 / R_{hm}$
- **$\Delta u$ (curvature half-spread):** $\Delta u = (u_{max} - u_{min}) / 2 = (R_{max} - R_{min}) / (2 \cdot R_{min} \cdot R_{max})$

The optimal Baerwald zeros in the radius domain are therefore:

$$\mathbf{R_1\ (inner) = 1 / (u_m + \Delta u \cdot (\sqrt{2} / 2)) = (2 \cdot R_{min} \cdot R_{max}) / [\ (R_{max} + R_{min}) + (\sqrt{2} / 2) \cdot (R_{max} - R_{min})\ ]}$$
$$\mathbf{R_2\ (outer) = 1 / (u_m - \Delta u \cdot (\sqrt{2} / 2)) = (2 \cdot R_{min} \cdot R_{max}) / [\ (R_{max} + R_{min}) - (\sqrt{2} / 2) \cdot (R_{max} - R_{min})\ ]}$$

Substituting the IEC values ($R_{min} = 60.325$ mm, $R_{max} = 146.05$ mm):

- $u_m = 0.0117066\ mm^{-1}$

- $\Delta u = 0.0048647\ mm^{-1}$
- **$R_1 = 1 / (0.0117066 + 0.0034399) = 66.02\ mm$** (66.00 mm with the non-linearized trigonometric equation).
- **$R_2 = 1 / (0.0117066 - 0.0034399) = 120.97\ mm$** (120.90 mm with the non-linearized trigonometric equation).

### 6.3 Analytic Solution of Loefgren B — Minimization of the $L_2$ Norm (Least Squares)

The Loefgren B criterion minimizes the effective (RMS) value of the error weighted with respect to the radius R (or with respect to the curvature u). Imposing the integral least-squares minimum condition over the normalized interval [-1, +1]:

$$\partial / \partial c_0,c_1 \int_{-1}^{+1} (x^2 + c_1 \cdot x + c_0)^2\, dx = 0$$

With uniform weighting in the normalized curvature x, the vertex of the parabola would remain at $u_m$ ($c_1 = 0$) and the minimum would give $c_0 = -1/3$, i.e. zeros at $x = \pm 1/\sqrt{3} \approx \pm 0.577$: the distance between the zeros would shrink by a factor of $\sqrt{(2/3)} \approx 0.816$ relative to Chebyshev. Loefgren's original formulation instead integrates along the radius R ($dR = du / u^2$), which gives more weight to the outer grooves: the vertex shifts toward lower curvatures ($u_v = 0.01140\ mm^{-1}$ versus $u_m = 0.01171\ mm^{-1}$) and the half-distance between the zeros is approx. $0.58 \cdot \Delta u$. The resulting IEC values are:

- **$R_1$ (Loefgren B, IEC) = 70.29 mm**
- **$R_2$ (Loefgren B, IEC) = 116.60 mm**

This brings the two Null Points closer together by approx. 8.6 mm overall, reducing the central peak of weighted error (between $R_1$ and $R_2$) by approx. one third relative to Baerwald, at the price of a larger error at the extremes (max WTE 0.212 °/cm versus 0.130 °/cm on a 9" tonearm).

### 6.4 Analytic Solution of Stevenson — Inner Boundary Constraint

Stevenson fixes the first zero exactly at the minimum recorded radius:

- **$u_1 = u_{max} \Longrightarrow R_1 = R_{min} = 60.325\ mm$ (IEC)**

and requires that the intermediate local maximum (at the vertex of the parabola $u_v = (u_1 + u_2) / 2$) be equal in magnitude to the value assumed at the outer edge $u_{min} = 1 / R_{max}$:

$$|W(u_v)| = |W(u_{min})|$$

Solving the algebraic equation for the second root $u_2$ as a function of $u_{min}$ and $u_{max}$:
$(u_{max} - u_2)^2 / 4 = (u_{min} - u_{max}) \cdot (u_{min} - u_2)$

Setting the normalized distance, the closed relation is obtained:
$u_2 = u_{max} - 2 \cdot (\sqrt{2} - 1) \cdot (u_{max} - u_{min}) \approx u_{max} - 0.828427 \cdot (u_{max} - u_{min})$

Substituting the IEC parameters:

- **$R_1 = 60.325\ mm$**
- **$R_2 = 117.42\ mm$**

## 7. Applied Appendix: Calculation Matrix for Real Reference Setups

The following develops the complete numerical model (mechanical, geometric and electrical) on four reference tonearms (SME 3012-R, Fidelity Research FR-64S, Mørch DP-8, SME 3009 S2 Improved) paired with a fleet of cartridges representative of the different technologies (very-low-impedance MC with integrated headshell, low/medium-impedance MC, Moving Iron and high-compliance Moving Magnet). The data for tonearms, cartridges and cables come from the manufacturers' datasheets [8–18].

### 7.1 Physical Parameters of the Tonearms Analyzed

1. **SME 3012-R (12 inches, damped thin-wall stainless steel armtube):**
   - Effective length ($L_{eff}$): 307.34 mm (12⅛", from the SME manual).
   - Pivot-to-Spindle distance (nominal SME $D_{p2s}$): 294.1 mm (11 9/16", from the SME manual; adjustable via the sliding base). With $L_{eff}$ = 307.34 mm this value corresponds to Baerwald.
   - Effective mass ($M_{eff}$): **14.0 g** (without cartridge, including the 7.5 g SME S2-R headshell; if the headshell is replaced with an integrated SPU G-shell, the bare armtube alone contributes approx. 6.5 g, est. value).
2. **Fidelity Research FR-64S (9.6 inches, high-inertia stainless steel with spring-based dynamic balancing):**
   - Effective length ($L_{eff}$): 245.0 mm.
   - Pivot-to-Spindle distance ($D_{p2s}$): 230.0 mm (nominal Overhang = 15.0 mm; Offset angle = 21.5°).
   - Effective mass ($M_{eff}$): **~31.0 g – 35.0 g** (including the original 16.2 g FR-S/3 headshell; approx. 19 g est. for the armtube alone without headshell, a figure not published by the manufacturer).
3. **Mørch DP-8 (9 inches, precision dual-pivot design with eccentric stabilizing masses and interchangeable armtubes):**
   - Effective length ($L_{eff}$): 230 mm with the 9" armtube (307.4 mm with the 12" armtube); for Baerwald $D_{p2s}$ = 211.9 mm.
   - Effective masses ($M_{eff}$) by armtube:
     - *Green Dot armtube:* **4.0 g** (ultra-light).
     - *Red Dot armtube:* ***6.0 g*** *(medium; some sources indicate 7 g*).
     - *Yellow Dot armtube:* ***8.0 g*** *(heavy*).
     - *Blue Dot armtube:* **14.0 g** (heavy Precision).
4. **SME 3009 Series II Improved (9 inches, aluminum armtube, ultra-low mass):**
   - Effective length ($L_{eff}$): 229.0 mm ($D_{p2s}$ = 215.4 mm).
   - Effective mass ($M_{eff}$): **6.5 g** (Fixed Headshell version) / **9.5 g** (S2 Detachable Headshell version). For Baerwald the sliding base must be set to $D_{p2s}$ = 210.9 mm.

## 7.2 Physical and Electrical Parameters of the Cartridges Analyzed

| Cartridge | Type and Stylus Profile | Body Mass $M_c$ (g) | Stated Compliance | Effective Compliance at 10 Hz ($C_{10}$) | Internal Impedance $R_c$ / Inductance $L_c$ | Nominal Output (1 kHz, 5 cm/s) | Nominal VTF (g) |
|---|---|---|---|---|---|---|---|
| **Ortofon SPU Classic GM MkII** | Low-Output MC (Conical 18 µm, integrated G-shell) | 30.0 g (GM; the GE weighs 28 g) | 8 µm/mN (at 10 Hz) | **8.0 µm/mN** | **2 Ω** (6 Ω earlier series) / ~2.5 µH | 0.20 mV | 4.0 g (3.0 – 5.0 g) |
| **Fidelity Research FR-7** | Low-Output MC, two-magnet push-pull generator (Elliptical 7.6×15.2 µm, integrated shell) | 30.0 g (integrated) | $6\times10^{-6}$ cm/dyne (100 Hz; FR-7f: $7\times10^{-6}$) → ~10.5–13 cu at 10 Hz | **~10.5 – 13 µm/mN** | **2 Ω** / ~2 µH | 0.20 mV | 2.5 g (2.0 – 3.0 g) |
| **Hana SL Mono** | Low-Output MC (Shibata on aluminum cantilever) | 5.0 g | $10\times10^{-6}$ cm/dyne (100 Hz) | **~16.0 – 17.5 µm/mN** | **30 Ω** (first series; MkII: 23 Ω, 8.6 g, 0.4 mV) / ~28 µH | 0.50 mV | 2.0 g |
| **Koetsu Onyx Platinum** | Low-Output MC (Onyx body, Sugano Line Contact stylus) | 12.5 g | n/a (not published; est. $5\times10^{-6}$ cm/dyne at 100 Hz) | **~8.5 – 9.0 µm/mN** | **~5 Ω** (est.: figure for the Rosewood Signature Platinum) / ~5 µH | 0.30 mV (0.4 mV std series) | 1.9 g (1.8 – 2.0 g) |
| **Kiseki PurpleHeart N.S.** | Low-Output MC (Amaranth wood body, Line Contact on boron) | 7.0 g | 16 µm/mN (at 10 Hz) | **16.0 µm/mN** | **42 Ω** / ~38 µH | 0.48 mV | 2.2 g (2.0 – 2.4 g) |
| **Nagaoka MP-700** | MI Permalloy (MicroRidge on boron) | 8.0 g | n/a (not published; est. $8.5\times10^{-6}$ cm/dyne at 100 Hz) | **~15.0 µm/mN** (est.) | **n/a / n/a (est. ~500–580 mH)** | 4.0 mV | 1.4 g |
| **Shure V15 Type III** | High-Compliance MM (Elliptical / VN35MR MicroRidge) | 6.3 g | $30\times10^{-6}$ cm/dyne (static, Shure); ~$22\times10^{-6}$ dynamic | **~22.5 µm/mN** | **1350 Ω / 500 mH** | 3.5 mV | 1.0 g (0.75 – 1.25 g) |

## 7.3 Mechanical ($f_0$), Geometric and Electrical Calculation Matrix for Specific Combinations

| Tonearm + Cartridge Combination | Total Mass Calculation $M_{tot}$ (g) | Resonance Frequency $f_0$ (Hz) | Recommended Geometric Alignment ($D_{p2s}$ / Null Points) | Optimal Electrical Load (SUT or Active Phono Preamp) | Engineering Assessment |
|---|---|---|---|---|---|
| **1. SME 3012-R + Hana SL Mono** (with SME S2-R headshell + 2.5 g spacer/screws) | $M_{eff}$ (14.0) + $M_c$ (5.0) + $M_h$ (2.5) = **21.5 g** | With $C_{10}$ = 17 cu: $f_0$ = 159.15 / √(21.5 × 17) = **8.32 Hz** (With $C_{10}$ = 16 cu: **8.58 Hz**) | **Loefgren A (Baerwald):** $D_{p2s}$ = 294.1 mm, O = 13.3 mm, $R_1$ = 66.0 mm, $R_2$ = 120.9 mm. | **$R_c$ = 30 Ω (first series):** active load recommended by Hana **≥ 400 Ω** (attenuation < 0.7 dB). With SUT: ratio **1:10 (470 Ω reflected)**. | **Excellent for Modern Monos.** To raise $f_0$ toward 9.5 Hz an ultralight 5 g headshell can be used ($M_{tot}$ = 19.0 g → $f_0$ = 8.9 Hz). |
| **2. SME 3012-R + Ortofon SPU Classic GM** (direct mounting without S2-R) | $M_{armtube}$ (6.5, est.) + $M_{SPU}$ (30.0) = **36.5 g** (requires additional SPU counterweight) | With $C_{10}$ = 8 cu: $f_0$ = 159.15 / √(36.5 × 8) = **9.31 Hz** | **Stevenson:** $D_{p2s}$ = 295.6 mm (O = 11.7 mm), $R_1$ = 60.3 mm, $R_2$ = 117.4 mm. With the manual's $D_{p2s}$ (294.1 mm), Baerwald is obtained instead. | **$R_c$ = 2 Ω:** With SUT ratio **1:26 ÷ 1:36** ($R_{ref}$ = 36 Ω – 69 Ω) or **Active Preamp at 20 – 50 Ω** (or Current-Mode). | **Absolute Reference.** Perfect mechanical synergy ($f_0$ = 9.31 Hz, in the middle of the window). |
| **3. Fidelity Research FR-64S + Fidelity Research FR-7** | $M_{armtube}$ (19.0) + $M_{FR7}$ (30.0) = **49.0 g** | With $C_{10}$ = 10.5 cu: $f_0$ = 159.15 / √(49.0 × 10.5) = **7.02 Hz** (with $C_{10}$ = 13 cu: **6.31 Hz**) | **Original FR Geometry / Stevenson:** $D_{p2s}$ = 230.0 mm (O = 15.0 mm), which coincides with Stevenson IEC ($D_{p2s}$ = 230.1 mm, O = 14.9 mm). | **$R_c$ = 2 Ω:** dedicated very-low-impedance SUT (e.g. ratio **1:30 → 52 Ω reflected**, or dedicated 2–3 Ω winding). | **Dedicated Historical Pairing**, but with $f_0$ below the 8–12 Hz window. The high mass blocks any parasitic chassis resonance; it requires pulley/belt-drive turntables on a rigid plinth free of modes at 6–7 Hz. |
| **4. Fidelity Research FR-64S + Koetsu Onyx Platinum** (with 12 g headshell + 1 g screws) | $M_{armtube}$ (19.0) + $M_{hs}$ (12.0) + $M_c$ (12.5) + $M_h$ (1.0) = **44.5 g** | With $C_{10}$ = 8.5 cu: $f_0$ = 159.15 / √(44.5 × 8.5) = **8.18 Hz** | **Loefgren A (Baerwald):** Set $D_{p2s}$ = **228.1 mm** (O = 16.9 mm) to obtain $R_1$ = 66.0 mm, $R_2$ = 120.9 mm. | **$R_c$ = 5 Ω:** With SUT ratio **1:20 (117.5 Ω reflected)** or **Active Preamp between 50 Ω and 100 Ω**. | **Excellent.** Replacing the original 16.2 g FR headshell with a 10–12 g ebony/magnesium one keeps $f_0$ above 8.2 Hz. |
| **5. Mørch DP-8 (14 g Blue armtube) + Kiseki PurpleHeart N.S.** | $M_{eff}$ (14.0) + $M_c$ (7.0) + $M_h$ (1.0) = **22.0 g** (or **16.0 g** with the 8 g Yellow armtube, 14.0 g with the 6 g Red armtube) | Blue armtube (14 g): **8.48 Hz**. Yellow armtube (8 g): $f_0$ = 159.15 / √(16 × 16) = **9.95 Hz**. Red armtube (6 g): 10.63 Hz | **Loefgren B or Baerwald:** Baerwald with $D_{p2s}$ = 211.9 mm, O = 18.1 mm, α = 23.97° (Loefgren B: $D_{p2s}$ = 211.4 mm). | **$R_c$ = 42 Ω:** Requires a high load, **400 Ω – 1000 Ω** in active mode, or SUT **1:10 (470 Ω reflected)**. Avoid a 1:20 SUT (117 Ω chokes the dynamics). | **Yellow armtube (8 g) Winner:** brings $f_0$ to **9.95 Hz**, in the middle of the window; the Red armtube (6 g) gives 10.6 Hz and the Blue armtube drops to 8.5 Hz. |

| | | | | | |
|---|---|---|---|---|---|
| **6. Mørch DP-8 (8 g Yellow armtube) + Nagaoka MP-700** | $M_{eff}$ (8.0) + $M_c$ (8.0) + $M_h$ (1.0) = **17.0 g** | With $C_{10} \approx 15$ cu (est.: Nagaoka does not publish the compliance): $f_0 = 159.15 / \sqrt{(17.0 \times 15)} =$ **9.97 Hz** | **Loefgren A (Baerwald):** $D_{p2s} = 211.9$ mm, $R_1 = 66.0$ mm, $R_2 = 120.9$ mm; rigorous SRA at 92.0°. | **$R_{in}$ = 47 kΩ**, target total capacitance **$C_{tot}$ = 100 – 150 pF** (Nagaoka specifies 100 pF; with est. $L_c$ of 580 mH and 120 pF → $f_e = 19.08$ kHz). Low-capacitance cable (e.g. Mogami 2964, 65 pF/m). | **Ideal Alignment:** Mechanical resonance at 9.97 Hz and electrical resonance at 19.1 kHz for maximum extension of the MicroRidge on boron. |
| **7. SME 3009 S2 Improved + Shure V15 Type III** | $M_{eff}$ (6.5) + $M_c$ (6.3) + $M_h$ (0.7) = **13.5 g** | With $C_{10} \approx 22.5$ cu (dynamic): $f_0 = 159.15 / \sqrt{(13.5 \times 22.5)} =$ **9.13 Hz** (with the 9.5 g detachable headshell version: 8.26 Hz; the FD-200 damping trough still reduces $Q_m$) | **Baerwald:** $R_1 = 66.0$ mm, $R_2 = 120.9$ mm, with the sliding base at $D_{p2s} = 210.9$ mm (the nominal SME value of 215.4 mm gives a different geometry). | **$R_{in}$ = 47 kΩ**, **$C_{tot}$ = 400 – 450 pF** (the V15 Type III with $L_c$ = 500 mH specifically requires 400–500 pF to linearize the stylus mechanical peak at 11.2 kHz). | **1970s Classic:** Unlike modern MMs, which want low capacitance, the V15-III requires a high capacitive load (~450 pF) so as not to sound bright. |

## 8. References

### Technical Literature and Standards


**[1]** E. Löfgren, study of the non-linear distortion in record reproduction caused by the angular deviation of the pick-up, Akustische Zeitschrift, vol. 3, November 1938 (English title: “On the Non-Linear Distortion in the Reproduction of Phonograph Records Caused by Angular Deviation of the Pickup Needle”).

**[2]** H. G. Baerwald, “Analytic Treatment of Tracking Error and Notes on Optimal Pick-Up Design”, Journal of the Society of Motion Picture Engineers, vol. 37, no. 12, December 1941.

**[3]** J. K. Stevenson, “Pickup Arm Design”, Wireless World, May and June 1966.

**[4]** IEC 60098 (formerly IEC 98, 1958): standard on analog phonograph records and playback equipment.

**[5]** DIN 45547: German standard from which the minimum and maximum recording radii cited in §2.4 are derived.

**[6]** JIS S 8502:1973: Japanese standard on phonograph records.

**[7]** RIAA: standard equalization curve for record cutting and playback (1954).


### Manufacturer Datasheets (accessed November 2026)


**[8]** Ortofon, SPU Classic GE MkII: datasheet (ortofon.com).

**[9]** Fidelity Research, FR-7, FR-7f and FR-64S: catalog data (audio-database.com).

**[10]** Koetsu, Onyx: specifications (hifiverse.io).

**[11]** Hana (Excel Sound), SL Mono and SL Mono MkII: manufacturer specifications as published by distributors (Music Direct, Audio Advisor).

**[12]** Kiseki, Purple Heart NS: specifications (kjwestone.co.uk); reviews in The Absolute Sound and Audiophilia.

**[13]** Denon, DL-103: specifications (stereophile.com).

**[14]** Shure, V15 Type III: User Guide (pubs.shure.com).

**[15]** Nagaoka, MP-700: manufacturer specifications as published by distributors.

**[16]** SME, 3012-R: user manual (manualslib.com) and hifi-wiki.com; SME 3009 Series II Improved: radiomuseum.org.

**[17]** Mørch, DP-8: specifications (playstereo.com); Stereophile, “Analog Corner” no. 248.

**[18]** Mogami, W2964: cable specifications (bhphotovideo.com).